SRIM-Based Investigation of Heavy-Ions ^{238}U, ^{132}Xe, ^{84}Kr, ^{56}Fe and ^{40}Ar Energy Loss and Penetration in Silicon devices.

Summary (Abstract)

This article investigates the impact of heavy ions (^{38}U, ^{132}Xe, ^{84}Kr, ^{56}Fe, ^{40}Ar) on silicon device, which are essential in electronic and photovoltaic technologies. These devices, vulnerable to ionizing radiation (particularly in space or nuclear facilities), have their electrical and optical properties altered by interactions between the ions and the crystal lattice. Using the SRIM (*Stopping and Range of Ions in Matter*) software, the study simulates the energy loss of the ions to distinguish the contributions of electronic losses, dominant at high energy, and nuclear losses, responsible for crystal defects at low energy. It also determines the penetration depth, an important parameter for optimizing the thickness of a silicon device.

Keywords: Ionizing radiation, Electronic and nuclear energy losses, SRIM.

1. Introduction

Semiconductor materials, such as silicon, play an important role in modern technologies, particularly forsilicon devices like solar cells. However, when exposed to extreme environments such as space or nuclear facilities, their performance can be significantly impaired by damage induced by ionizing radiation. This damage results primarily from the interaction between incident ions and the crystal lattice of the semiconductor material, leading to a degradation of the electrical and optical properties of silicon devices[1] [2] .

In this context, studying the energy loss mechanisms of heavy ions in silicon allows us to assess the impact of these ions on the material's structure and to model their influence on the production of crystal defects [3] [4] . Ionic energy losses can be electronic or nuclear in nature.

In this work, we investigate the interaction of heavy ions ^{238}U, ^{132}Xe, ^{84}Kr, ^{56}Fe, and ^{40}Ar with a silicon device using the SRIM (Stopping *and Range of Ions in Matter)* software. We will first quantify the respective contributions of electronic and nuclear energy losses as a function of the incident ion energy, and then determine the stopping power and penetration range of these ions in silicon, in order to assess their depth of interaction with the material. [5] [6] [7] [8] [9].

2. Study of the loss of ionic energy in the silicon device

When heavy ions enter the silicon device, they cause two types of energy loss:
The loss of electronic energy,which corresponds to the transfer of energy from the ion to the electrons of the target material.
The loss of nuclear energy, characterized by direct collisions between the ion and the atomic nuclei of the crystal lattice.

These mechanisms, whose relative importance varies with the incident energy, jointly determine the degradation of the silicon performance. They can be characterized by the following two relationships: [9][10]

$$LET = \frac{1}{r}.\frac{dE}{dx} \quad (I)$$

Where $\frac{dE}{dx}$: is the energy deposited by the ionizing particle when it passes through the material (silicon).

r : is the density, that is, the mass per unit volume.

The LET consists of two fundamental parts: one due to electronic interactions, the other to nuclear interactions. [11]

$$LET = LETnucleaire + LETelectronique \quad (II)$$

a. Electronic energy losses:

The electronic energy losses of heavy ions in silicon arise mainly from inelastic interactions between the incident ion and the electrons of the crystal lattice.

During their passage, these ions transfer a significant fraction of their kinetic energy to electrons in the target (silicon), causing excitation and ionization processes. [12]

This transfer is described, in SRIM, by a modified form of the Bethe equation, adapted to heavy ions through the introduction of a dynamic effective charge: [13] [14] [15] [16]

$$\left(\frac{dE}{dx}\right)_e = \frac{4\pi e^4 Z_{eff}^2}{m_e c^2 \beta^2} n_e \left[\ln\left(\frac{2 m_e c^2 \beta^2}{I}\right) - \beta^2 \right] \quad (III)$$

Or n_e is the electron density of silicon, I ≈ 173 eV its average ionization potential, $\beta = \frac{v}{c}$ the reduced velocity of the ion, and the effective charge given by Z_{eff} Ziegler's semi-empirical expression : [17]

$$Z_{eff} = Z_1 \left(1 - e^{-125\beta/Z_1^{2/3}}\right) \quad (IV)$$

Or Z_1 is the atomic number of the ion

This intense electronic braking generates a high energy density along the ion's trajectory, leading to the creation of numerous electron- -hole pairs. When this density exceeds a critical threshold, it can induce irreversible changes in the crystal structure: formation of point defects, dislocations, and in some cases, local amorphization of silicon.

Beyond -structural effects, these electronic losses also alter the electrical properties of the semiconductor. They lead to a decrease in carrier mobility, the appearance of non-radiative recombination centers, and a degradation of overall conductivity. These changes are particularly critical for microelectronic and photovoltaic devices, whose performance relies on material stability. [18]

We also studied nuclear losses, which result from direct collisions between heavy ions and silicon nuclei.

b. Nuclear energy losses

Nuclear energy losses in silicon result from direct elastic collisions between incident ions and the material's nuclei. Unlike electronic losses, which involve electrons in the crystal lattice, these nuclear interactions transfer some of the ion's kinetic energy to the silicon atoms, causing them to move out of their crystal sites. This mechanism leads to the formation of point defects such as vacancies and interstitials, disrupting the crystal order. [19]

In SRIM, nuclear braking is described by the universal ZBL (Ziegler–Biersack–Littmark) model**,** based on an interaction potential.

Nuclear loss is written: [20] [21]

$$\left(\frac{dE}{dx}\right)_n = \frac{4\pi Z_1 Z_2 e^4}{M_1}\frac{M_1 M_2}{\left(M_1+M_2\right)^2}\frac{1}{E}S_n\left(\in\right) \text{(V)}$$

where Z_1 and Z_2 are the atomic numbers of the ion and silicon, M_1 And M_2 their masses, E the kinetic energy of the ion, and $S_n\left(\in\right)$ the reduced nuclear braking function, given by:

$$S_n\left(\in\right) = \frac{\ln\left(1+\varepsilon\right)}{2\left(\varepsilon + 0.01321\varepsilon^{0.21226} + 0.19593\varepsilon^{0.5}\right)} \text{(VI)}$$

with the reduced energy parameter:

$$S_n\left(\in\right) = \frac{32.53M_2}{\left(M_1+M_2\right)Z_1Z_2\left(Z_1^{2/3}+Z_2^{2/3}\right)^{1/2}}E \text{(VII)}$$

This model allows us to describe the energy transfer during ion-nucleus collisions, taking into account the electron screening effect which modifies the short-range Coulomb interaction.
Displaced atoms can initiate cascades of collisions, where each ejected atom in turn transfers energy to its neighbors, amplifying damage in a localized area. These processes lead to the formation of complex defects, dislocations, and even amorphous zones or microcracks.
Unlike electronic losses, which primarily affect electrical properties, nuclear losses mainly degrade the mechanical and crystallographic stability of the material. [16]

It is also important to study the stopping power and penetration range of the ions, essential parameters for quantifying the energy deposited and the depth of interaction in silicon

c. Ion stopping power and penetration range:

The penetration range or pathrepresents the total distance traveled by an ion in a material before its complete immobilization, marking the integral transfer of its kinetic energy into the target material. It is expressed by the following relation: [9]

$$\text{Parcours} = \int_0^{E_i} \frac{1}{\left(\frac{\Delta E}{\Delta x}\right)} . dE \quad \text{(VIII)}$$

E_i : is the initial kinetic energy of the ion when it enters the target material.

ΔE : the change in energy and Δx : is the change in position.

After conducting a study on energy losses, stopping power and penetration range of ions, we first analyze the evolution of these losses for different heavy ions, before interpreting the results obtained and discussing the impact of irradiation on the performance of the silicon device.

3. Results and Discussion

The study of the interaction of charged particles with silicon allowed us to evaluate the electronic and nuclear losses of the charged particles and the stopping power of silicon.
The results obtained are represented by tables showing numerical values of energy losses for various ions, at irradiation levels varying between 5 and 250 MeV.

Tables III-1, III-2 and III-3 give the results obtained respectively for E = 5 MeV, E = 100 MeV and E = 250 MeV

Table III-1 :Energy loss of ions (U, Xe, Kr, Iron and Ar) in Silicon for an irradiation energy of 5 MeV

Particles	Energy	Electronic energy loss	Energy lossnuclear	Total Energy Loss
Uranium		$1,193.10^{1}$	$1,014.\ 10^{1}$	22,700
Xenon		$9,721.10^{0}$	$3,354.10^{0}$	13,075
Krypton	5	$9,750.10^{0}$	$1,279.10^{0}$	11,029
Iron		$1,115.10^{1}$	$5,405.10^{-1}$	11,690
Argon		$1,059\ .10^{1}$	$2,169.10^{-1}$	10,807

Table III-2 :Energy loss of ions (U, Xe, Kr, Iron and Ar) in Silicon for an irradiation energy of 100 MeV

Particles	Energy	Electronic energy loss	Energy lossnuclear	Total Energy Loss
Uranium		$4,986.10^{1}$	$1,604.\ 10^{0}$	51,464
Xenon		$4,844.10^{1}$	$3,912.10^{-1}$	48,831
Krypton	100	$3,780.10^{1}$	$1,282.10^{-1}$	37,928
Iron		$2,925.10^{1}$	$4,948.10^{-2}$	29,299
Argon		$1,719\ .10^{1}$	$1,854.10^{-2}$	17,208

Table III-3 :Energy loss of ions (U, Xe, Kr, Iron and Ar) in Silicon for an irradiation energy of 250 MeV

Particles	Energy	Electronic energy loss	Energy lossnuclear	Total Energy Loss
Uranium	250	$8{,}145.10^{1}$	$7{,}879\ .10^{-1}$	82,238
Xenon		$6{,}482.10^{1}$	$1{,}845\ .10^{-1}$	65,005
Krypton		$4{,}066.10^{1}$	$5{,}918\ .10^{-2}$	40,719
Iron		$2{,}540.10^{1}$	$2{,}253\ .10^{-2}$	25,423
Argon		$1{,}244.10^{1}$	$8{,}351\ .10^{-3}$	12,448

The unit of irradiation energy is *MeV* and energy losses are in $Mev\ /\ mg.cm^{-2}$

The analysis of these tables allows us to analyze the variation profiles of electronic and nuclear energy losses of the ions: U, Xe, Kr, Iron and Ar

a. Analysis of Electronic Energy Losses

The figure below shows the electron loss profile as a function of irradiation energy for different heavy ions (U, Xe, Kr, Iron and Ar)

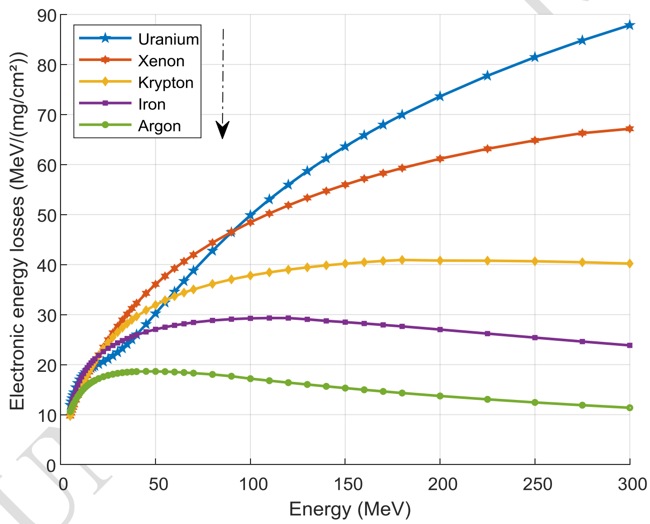

Figure III-1:*Electron energy loss by U, Xe, Kr, Fe and Ar ions in silicon as a function of irradiation energy from 5 to 300 MeV*

Figure III-1: shows a significant increase in electronic energy loss with ion energy for all elements considered**.**

The increase in energy losses observed particularly for uranium is mainly explained by its high effective atomic number (Z_{eff}).While heavier ions reach a state of equilibrium charge more quickly and exhibit saturation or relative decrease.

The increased electronic energy loss means that when the ion passes through silicon at higher energies, it interacts more with the electrons in silicon, resulting in a greater energy loss.

b. Analysis of Nuclear Energy Losses

The figure below illustrates the nuclear loss profile as a function of irradiation energy for different heavy ions (U, Xe, Kr, Iron and Ar)

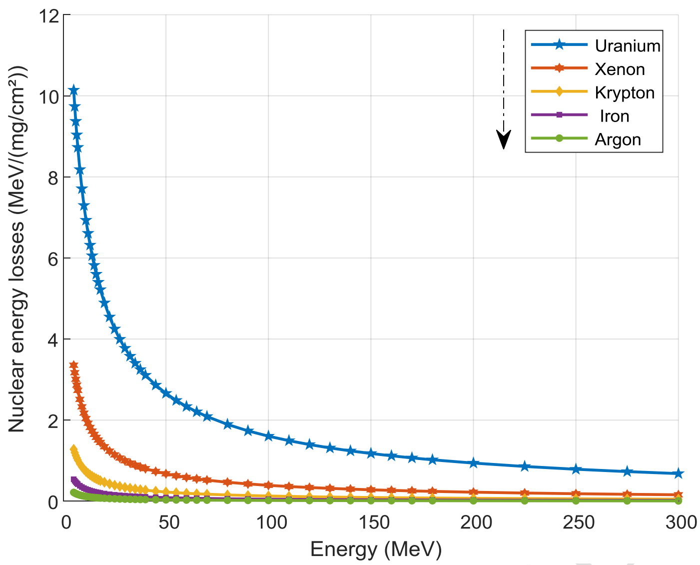

Figure III-2:*Nuclear energy loss by U, Xe, Kr, Fe and Ar ions in silicon as a function of irradiation energy from 5 to 300MeV*.

Figure III-2 This shows that, unlike electronic energy losses, nuclear energy losses decrease with ion energy. This is because, as the energy of the charged particles increases, interactions with silicon nuclei decrease as the ion rapidly traverses the lattice, resulting in little efficient energy transfer with the nuclei.

Uranium exhibits the highest nuclear energy loss at low energies ($11.93\, Mev / mg.cm^{-2}$ at $5MeV$), but it decreases rapidly as energy increases.

For the other elements, nuclear energy losses are relatively low across the entire energy range.

At higher energies, nuclear energy losses are negligible compared to electronic energy losses. This indicates that electronic interactions dominate the total energy loss of ions at higher energies.

Figures **III-1** and **III-2** show how different ions lose energy when they enter silicon. This energy loss occurs through electronic and nuclear interactions. The relative importance of these two mechanisms depends on the energy and type of the ions.

The analysis of electronic and nuclear energy losses leads us to consider the penetration path of ions in the target material.

Indeed, these mechanisms directly influence the depth of interaction of particles in the medium they pass through.

The following tables present numerical values of the penetration path for various ions, at irradiation levels of 5 MeV, 50 MeV, 100 MeV and 200 MeV obtained using the SRIM software.

Table III-4: Penetration path of ions (*U, Xe, Kr, Fe and Ar)*for irradiation energies of 5 and 50 MeV

Particles	Energy	Course	Energy	Course
Uranium	5	9892.10^{-4}	50	08.22
Xenon		1.82		09.62
Krypton		2.60		11.07
Iron		3.00		11.78
Argon		3.03		14.43

Table III-5: Penetration paths of ions (*U, Xe, Kr, Fe and Ar)* for irradiation energies of 100 and 200 MeV

Particles	Energy	Course	Energy	Course
Uranium	100	13.34	200	20.11
Xenon		14.61		22.34
Krypton		17.14		27.90
Iron		19.32		34.47
Argon		26.32		54.46

The unit for irradiation energy is in megaelectronvolts (*MeV*) and the penetration length in *μm*

c. Analysis of Ionic Penetration Profiles in Silicon:

The following figure shows the penetration depth (path) of different ions (U, Xe, Kr, Fe and Ar) in silicon as a function of their energy, ranging from 5 to 300 MeV.

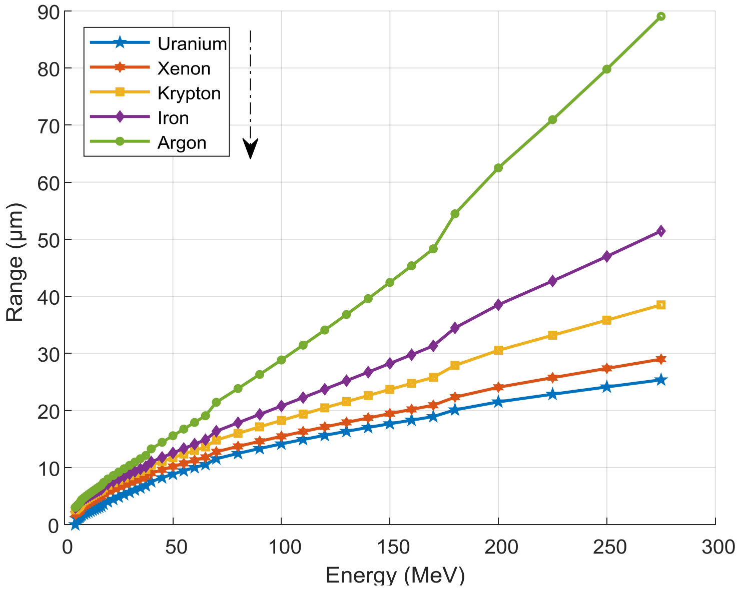

***Figure III-3**: Penetration profiles as a function of energy of U, Xe, Kr, Fe and Ar ionsin silicon.*

The ion's range increases with increasing energy. The higher the ion's energy, the deeper it penetrates the silicon.

The path length varies considerably depending on the nature of the ion. Argon has the longest path length (89.05 µm), followed by Iron, then Krypton, Xenon and Uranium (25.37 µm), which have much shorter path lengths for an irradiation energy range of 5 to 300 MeV. These results can be explained by the mechanisms of interaction between ions and matter: Heavy ions (Argon and Iron) lose their energy primarily through electronic interactions (excitation and ionization of silicon atoms). They experience less deflection and can therefore penetrate deeper.
In contrast, heavier ions (Krypton, Xenon, and Uranium) undergo more nuclear collisions (scattering by the atomic nuclei of silicon), which slows their progress and reduces their distance. They also deposit their energy closer to the surface.

d. Analysis of Electronic and Nuclear Energy Losses as a Function of Ion Penetration Depth:

Electronic and nuclear energy losses are fundamental phenomena that determine the behavior of ions when they penetrate a target material (Silicon).

The following tables present some numerical values of electronic, nuclear and penetration path losses for various ions, at various irradiation levels.

Table III-6 : Electron loss, nuclear loss and penetration path of ions (U, Xe, Kr, Fe and Ar) in siliconat irradiation levels of 5 MeV.

Particles	Energy	Electronic energyloss	Energy lossnuclear	Course
Uranium	5	$1,193.10^{1}$	$1,014.\,10^{1}$	9892.10^{-4}
Xenon		$9,721.10^{0}$	$3,354.10^{0}$	1.82
Krypton		$9,750.10^{0}$	$1,279.10^{0}$	2.60
Iron		$1,115.10^{1}$	$5,405.10^{-1}$	3.00
Argon		$1,059\ .10^{1}$	$2,169.10^{-1}$	3.03

Table III-7 : Electron loss, nuclear loss and penetration path of ions (U, Xe, Kr, Fe and Ar) in siliconat radiation levels of 100 MeV **.**

Particles	Energy	Electronic energy loss	Energy lossnuclear	Course
Uranium	100	$4,986.10^{1}$	$1,604.\,10^{0}$	13.34
Xenon		$4,844.10^{1}$	$3,912.10^{-1}$	14.61
Krypton		$3,780.10^{1}$	$1,282.10^{-1}$	17.14
Iron		$2,925.10^{1}$	$4,948.10^{-2}$	19.32
Argon		$1,719\ .10^{1}$	$1,854.10^{-2}$	26.32

Table III-8: Electron loss, nuclear loss and penetration path of ions (U, Xe, Kr, Fe and Ar) in siliconat irradiation levels of 250 MeV **.**

Particles	Energy	Electronic energy loss	Energy lossnuclear	Course
Uranium	250	$8,145.10^{1}$	$7,879\ .10^{-1}$	22.85
Xenon		$6,482.10^{1}$	$1,845\ .10^{-1}$	25.75
Krypton		$4,066.10^{1}$	$5,918\ .10^{-2}$	33.18
Iron		$2,540.10^{1}$	$2,253\ .10^{-2}$	42.69
Argon		$1,244.10^{1}$	$8,351\ .10^{-3}$	70.95

The unit for irradiation energy is in megaelectronvolts (MeV), for ion energy losses in $Mev\,/\,mg.cm^{-2}$ and penetration length in µm.

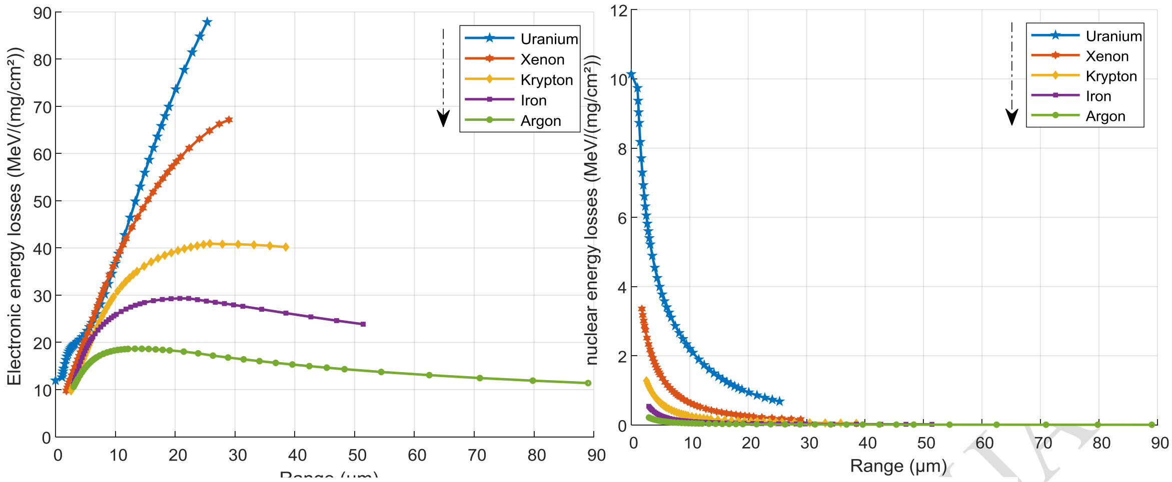

Figure III-4 *:Loss of electronic and nuclear energy as a function of the penetration of U, Xe, Kr, Fe and Ar ionsin silicon*

We observed that the loss of electronic energy initially increases with the path length and then tends to stabilize or even decrease slightly after a certain distance. This contrasts with the loss of nuclear energy, which decreases rapidly with increasing path length for all the ions considered.

However, these variations are explained by a strong interaction between the incident ion and the electrons of silicon at the beginning of its journey. This interaction gradually decreases as the ion loses kinetic energy, resulting in a change in its effective charge.

e. Analysis of total energy losses as a function of the thickness traversed

The evolution of total energy losses as a function of the thickness traversed allows us to identify the region of silicon where each ion deposits the majority of its energy before stopping. The following figure illustrates these variations for U, Xe, Kr, Fe, and Ar ions.

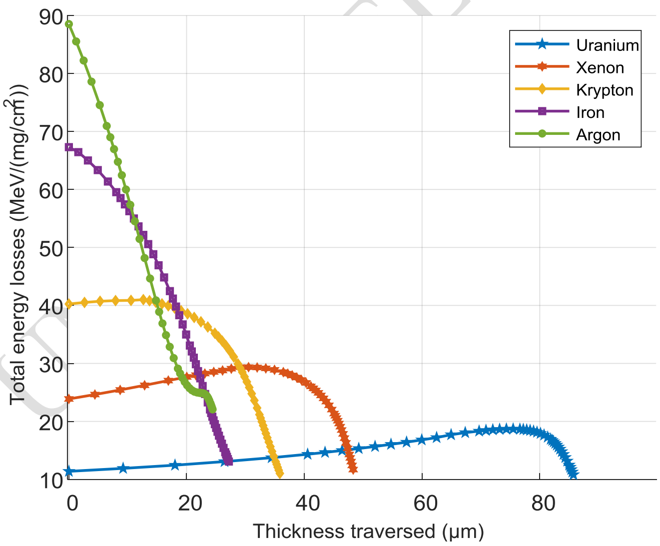

Figure III -5: *Total energy losses as a function of the thickness traversed for U, Xe, Kr, Fe and Ar ions in silicon.*

The profiles show that the ions lose more and more energy as they move through the material, then stop at a very specific depth: argon reaches 85.72 µm, iron 48.30 µm, krypton 35.84 µm, xenon 27.18 µm, and uranium only 24.42 µm.

These results confirm that the heavier the ion, the closer it deposits its energy to the surface, which is critical for the degradation of the active layers of silicon devices.

f. Analysis of total energy losses as a function of ion velocity

The ion's velocity directly influences the electronic and nuclear braking mechanisms. Studying the total losses as a function of velocity allows us to identify the dominant interaction regimes.

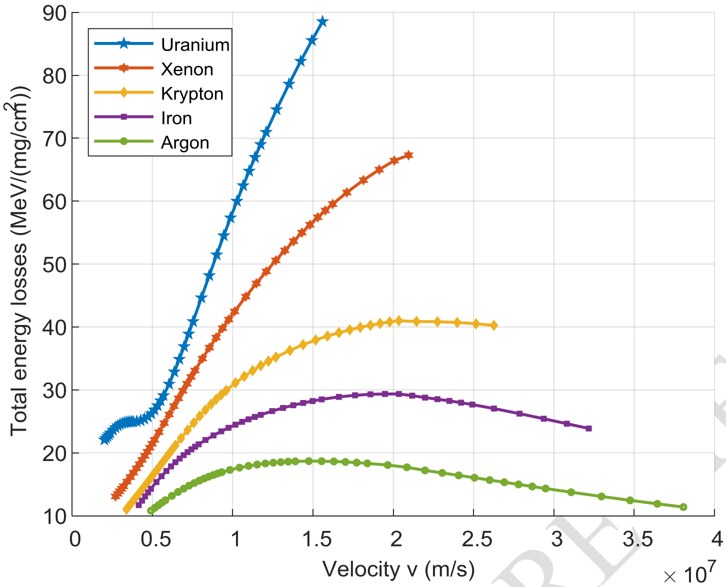

Figure III -6: *Total energy losses as a function of the velocity of U, Xe, Kr, Fe and Ar ions in silicon.*

Figure III -6shows two clear trends: for uranium, xenon and krypton, energy losses increase with speed due to the rise in their effective charge, which strengthens electronic interactions.
Conversely, iron and argon show a peak followed by a decline, a sign of the transition from a regime dominated by low-speed nuclear collisions to a high-speed electronic regime.
This maximum represents the point where their effective charge reaches its highest level before decreasing slightly at very high speed.

g. Analysis of the evolution of the effective load as a function of speed

The effective charge $Z_{eff}(v)$ is a key parameter in describing electronic losses. According to the modified Bethe equation, the electronic loss is proportional to $(Z_{eff})^2$.
The following figure illustrates its evolution as a function of speed.

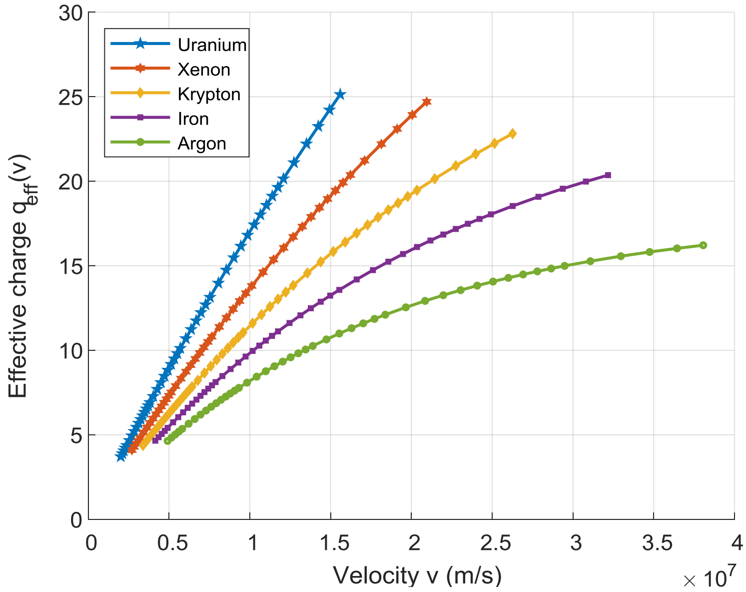

Figure III -7: *Effective charge Z_{eff} of U, Xe, Kr, Fe and Ar ions as a function of velocity.*

Figure III -7shows that the effective charge increases with speed for all ions, but much more markedly for heavy ions such as uranium, xenon and krypton, which reach significantly higher values than iron and argon.

Uranium actually exhibits the fastest growth, which explains its particularly high electron losses.

Conversely, light ions show only a moderate increase in their effective charge, a sign of weaker ionization of silicon.

The whole confirms that electronic losses dominate at high speeds, while nuclear losses remain predominant at low speeds, in accordance with the Bethe and ZBL models.

5. Conclusion and Perspectives

This study, using simulations performed with the SRIM software, analyzed the energy loss mechanisms and penetration range of heavy ions (^{238}U, ^{132}Xe, ^{84}Kr, ^{56}Fe, and ^{40}Ar) in silicon. The results highlighted several key points:

the predominance of high-energy electronic losses, mainly related to Coulomb interactions with the electrons of the material;

the increasing importance of low-energy nuclear losses, responsible for the creation of defects in the crystal lattice;

penetration depths vary depending on the nature and energy of the ions, which opens up perspectives for optimizing the thickness of electronics components and photovoltaic devices.

These observations highlight both the properties of the incident ions and the characteristics of the target material in order to better predict and mitigate radiation-induced damage.

To extend this work, several research perspectives can be considered:

- validation of simulation results through controlled irradiation experiments;

- the extension of the study to other ions or other semiconductor materials, such as GaAs or SiC, for specific applications;
- the integration of multi-scale modeling approaches to establish a link between microscopic damage induced by irradiation and the macroscopic performance for photovoltaic applications for example.

Thus, this work contributes to a better understanding of the effects of irradiation on silicon devices and paves the way for the development of more resistant and efficient electronics components and photovoltaic devices, particularly for applications in extreme environments.

References

[1] S. Mishra, K. Bhargava, and D. Deb, “Numerical simulation of potential induced degradation (PID) in different thin-film solar cells using SCAPS-1D,” *Solar Energy* , vol. 188, p. 353 - 360, August 2019, doi: 10.1016/j.solener.2019.05.077.

[2] MJ Hossain, M. Sun, and KO Davis, “Photon management in silicon photovoltaic cells: A critical review,” *Solar Energy Materials and Solar Cells* , vol. 267, p. 112715, Apr. 2024, doi: 10.1016/j.solmat.2024.112715.

[3] D. Mitina, E. Verbitskaya, I. Eremin, and N. Fadeeva, “Prediction of radiation degradation of Si detectors irradiated by relativistic ions of different masses”, *J. Phys.: Conf. Ser.* , flight. 2103, no ˙ 1, p. 012068, Nov. 2021, doi: 10.1088/1742-6596/2103/1/012068.

[4] A. Fedoseyev, M. Turowski, T. Bald, A. Raman, and JH Warner, “Radiation effects on solar cells: experiments, models, and simulations: DLTS vs. SRIM for trap data”, in *Nanophotonics and Macrophotonics for Space Environments VII* , SPIE, September 2013, p. 239 – 252. doi: 10.1117/12.2025405.

[5] GP Adhikari and HK Limbu, “Damage Formation and Calculation of Energy Loss during Implantation of Antimony and Boron Ion in Silicon Target”, *Journal of Nepal Physical Society* , vol. 5, no ˙ 1, p. 103 - 110, Dec. 2019, doi: 10.3126/jnphyssoc.v5i1.26939.

[6] F. Sikler, “A simple energy loss model and its applications for silicon detectors”, *Nuclear Instruments and Methods in Physics Research Section A: Accelerators, Spectrometers, Detectors and Associated Equipment* , vol. 691, p. 16 - 29, Nov. 2012, doi: 10.1016/j.nima.2012.06.064.

[7] FA Houle, “Adaptive response by an electrolyte: resilience to electron losses in a dye-sensitized porous photoanode”, *Chem. Sci.* , flight. 12, no ˙ 17, p. 6117 - 6128, May 2021, doi: 10.1039/D1SC00384D.

[8] U. Aeberhard, “Simulation of Nanostructure-Based High-Efficiency Solar Cells: Challenges, Existing Approaches, and Future Directions,” *IEEE Journal of Selected Topics in Quantum Electronics* , vol. 19, no ˙ 5, p. 1 - 11, Sept. 2013, doi: 10.1109/JSTQE.2013.2257701.

[9] I. Gaye, S. Yanhdet, D. Gaye, A. Diallo, AS Bouzou, and M. Wade, “SRIM simulation of the interaction of heavy ions 36Ar, 78Kr, 136Xe and 238U with silicon material,” vol. 37, no. 3 , 2022.

[10] MOE-Ghossain, “Calculations of Stopping Power, and Range of Ions Radiation (Alpha Particles) Interaction with Different Materials and Human Body Parts”, *International Journal of Physics* , vol. 5, no. 3, p. 92 - 98, May 2017, doi: 10.12691/ijp-5-3-5.

[11] A. Javanainen *et al.* , “Linear energy transfer of heavy ions in silicon”, *IEEE Transactions on Nuclear Science* , p. 1158 - 1162, 2007, doi: 10.1109/TNS.2007.895121

[12] JJ Grob et al., Energy loss of heavy ions in nuclear collisions in silicon, Phys. Rev. B 11, 3273 (1974).

[13] H. Bethe, Zur Theorie des Durchgangs schneller Korpuskularstrahlen durch Materie, Annalen der Physik, 1930.

[14] H. Bethe, Bremsformel für Elektronen relativistischer Geschwindigkeit, Zeitschrift für Physik, 1932.

[15] JF Ziegler, Stopping of Energetic Light Ions in Elemental Matter, J. Appl. Phys. 85, 1249 (1999).

[16] JF Ziegler, JP Biersack, U. Littmark, The Stopping and Range of Ions in Solids, Pergamon Press, 1985

[17] F. Salvat, Bethe stopping-power formula and its corrections, Phys. Rev. At 106, 032809 (2022).

[18] ZG Wang et al., *Amorphization of silicon under ion irradiation: mechanisms and thresholds* , Nucl. Instrument. Methods Phys. Res. B 286, 98–104 (2012).

[19] Lindhard J., Scharff M., Schiøtt HE, Range concepts and heavy ion ranges in matter, Mat. Fys. Medd. Dan. Vid. Selsk. 33, 1 (1963).

[20]JF Ziegler, JP Biersack, U. Littmark **,** *The Stopping and Range of Ions in Solids* , Pergamon Press, 1985.

[21]JP Biersack & L. Haggmark , *A Monte Carlo Computer Program for the Transport of Energetic Ions in Amorphous Targets* , Nucl. Instrument. Methods 174, 257 (1980).